

Docking-based 3D-QSAR study for selectivity of DPP4, DPP8, and DPP9 inhibitors

Nam Sook Kang,* Jin Hee Ahn, Sung Soo Kim, Chong Hak Chae and Sung-Eun Yoo

Korea Research Institute of Chemical Technology, Yuseong-Gu, Daejeon 305-600, Republic of Korea

Received 21 December 2006; revised 19 March 2007; accepted 10 April 2007

Available online 13 April 2007

Abstract—In order to obtain information regarding the design of selective DPP4 inhibitors, a 3D-QSAR study was conducted using DPP4, DPP8, and DPP9 inhibitors including newly synthesized six- and seven-membered cyclic hydrazine derivatives (KR64300, KR64301), which were evaluated in vitro for their inhibition of DPP4, DPP8, and DPP9. In this study, a highly predictive CoMFA model based on the fast-docking for DPP4, DPP8, and DPP9 inhibitors was obtained. This reliable model showed leave-one-out cross-validation q^2 and conventional r^2 values of 0.68 and 0.96 for the DPP4 inhibitors, 0.58 and 0.98 for the DPP8 inhibitors, and 0.68 and 0.97 for the DPP9 inhibitors, respectively. The validation of the CoMFA model was confirmed by the compounds in the test set, including the synthesized six- and seven-membered cyclic hydrazines. According to this study, to obtain selective DPP4 inhibitors compared to their isozymes, the interaction of the inhibitors with the S3 site and S1' site in DPP4 must be considered. The proposed newly synthesized compounds, KR64300 and KR64301, interact well with the sites mentioned above, showing excellent selectivity.

© 2007 Elsevier Ltd. All rights reserved.

DPP4 is a serine protease which cleaves the N-terminal dipeptide with a preference for Xaa-Pro or Xaa-Ala.¹ Recently, DPP4 has become known as a promising new target for the treatment of Type 2 diabetes mellitus.² Inhibition of DPP4 increases the level of circulating glucagon-like peptide 1 (GLP-1), an incretin hormone stimulating glucose-dependent insulin biosynthesis and secretion, and thus increases insulin secretion,³ which can ameliorate hyperglycemia in Type 2 diabetes. A number of orally active inhibitors of DPP4 have been reported in the literature⁴ and several compounds including Vildagliptin (LAF237)⁵ and Sitagliptin (MK-0431)⁶ are in late clinical development, and the first inhibitors may reach the market within 3–4 years. However, potential side-effects associated with DPP4 inhibitors may result from the inadvertent inhibition of related enzymes. As mentioned earlier, DPP4 belongs to a group of serine proteases, of which the physiological importance is largely unknown. The enzymes most closely related to DPP4 are the fibroblast activation protein-(FAP), DPP-II, DPP8, and DPP9.⁷ Although the precise physiological functions of the enzyme are not known, DPP8 and DPP9 are widely distributed cytosolic en-

zymes, and their inhibition has been suggested to be responsible for at least some of the toxic effects of DPP4 inhibitors identified to date, including alopecia, thrombocytopenia, anaemia, enlarged spleen, multiple histological pathologies, and animal mortality.⁸ Consequently, DPP4 inhibitors should demonstrate high selectivity against other peptidases mentioned above, in particular DPP8 and DPP9.

For these reasons, a 3D-QSAR study was conducted to examine the structural characteristics according to DPP isozymes. In addition, the aligned conformations set up for 3D-QSAR study were obtained from a docking study in order to demonstrate the interaction between inhibitors and DPP isozymes including DPP4, DPP8, and DPP9. The experimental team conducting this study synthesized the cyclic hydrazine derivatives (KR64300, KR64301), including the trifluoro-benzene group like MK0431. These were evaluated in vitro for their inhibition of DPP4, DPP8, and DPP9 in order to obtain small molecules showing DPP4 selective biological activity. Using the 3D-QSAR, the inhibitory activity of the new inhibitors was predicted, and this was compared to the experimental values.

Tables 1 and 2 show a series of DPP isozyme inhibitors originally published by Weber et al. in 2005,⁹ which were divided into a training set and a test set. The training set

Keywords: DPP4; DPP8; DPP9; Selectivity; 3D-QSAR.

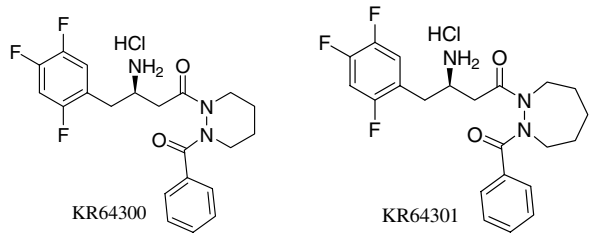
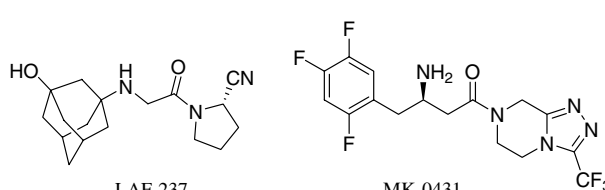
* Corresponding author. Tel.: +82 42 860 7452; fax: +82 42 860 7635; e-mail: nskang@kriict.re.kr

Table 1. The 43 compounds used in a training set (Ref. 9)

Compound ²	DPP4-obs	DPP8-obs	DPP9-obs
01-45	5.60	4.62	4.20
01-46	5.96	4.68	4.19
01-49	5.74	4.15	4.00
01-51	5.46	4.74	4.62
01-52	5.80	5.03	4.57
01-56	5.57	4.66	4.30
01-57	5.11	4.21	4.00
01-58	5.82	4.24	4.00
01-61	6.14	4.49	4.59
01-63	5.80	4.96	4.47
01-64	6.07	5.24	4.44
01-65	5.23	4.00	4.00
01-66	5.32	5.15	4.70
01-68	5.44	5.37	5.11
01-69	5.59	5.52	5.02
01-70	5.42	5.48	5.29
01-71	5.89	5.49	5.19
01-73	6.24	4.20	4.00
01-74	6.59	4.80	4.37
01-75	6.89	4.75	4.55
01-76	7.85	5.07	4.60
02-02	5.38	5.66	5.80
02-03	5.34	6.66	6.49
02-04	5.01	4.00	4.00
02-12I	4.55	4.24	4.47
02-12M	5.44	4.21	4.17
02-12Q	5.92	4.07	4.00
02-12T	4.77	4.20	4.00
02-12Y	5.24	4.24	4.00
02-21	5.96	4.64	4.35
02-23	6.57	4.00	4.23
02-24	6.00	4.41	4.43
02-25	6.19	4.06	4.07
02-35	6.22	4.38	4.32
02-39	6.02	4.33	4.25
02-40	5.96	4.77	4.24
02-43	7.22	4.00	4.28
03-32	7.04	4.82	4.21
03-38	7.12	4.66	4.18
03-40	6.57	5.10	4.34
03-41	7.04	4.89	4.59
03-47	6.68	4.85	4.09
03-49	6.37	6.34	4.24

comprises of 43 compounds. The test set, which was randomly selected, consisted of 10 compounds including LAF237 and MK0431 in late clinical development and the proposed new inhibitors, KR64300 and KR64301. The in vitro activities for DPP4, DPP8, and DPP9 of the LAF237, MK0431, KR64300, and KR64301 compounds were estimated by the biological experimental team conducting this study.¹⁰ The in vitro activities, IC_{50} , were transformed into pIC_{50} ($-\log IC_{50}$) and used as dependent variables in the CoMFA calculations. 3D structures of β -amino group derivatives were built using an in-house co-crystal structure of KR64301 with DPP4 (2OLE.pdb)¹⁰ and the Brookhaven Protein Databank, 1X70.pdb.¹¹ Conversely, to prepare the 3D structures of the selected compounds having α -amino groups, DPP4-inhibitor complex structures were used in the Brookhaven Protein DataBank, 1NU8.pdb¹² and 1ORW.pdb.¹³ From these complex structures, inhibitor structures were extracted and 3D structures were con-

Table 2. The 10 compounds used in a test set

			
			
Test set ^c	DPP4-obs	DPP8-obs	DPP9-obs
01-54	5.66	4.25	4.00
01-60	6.41	5.00	4.89
01-67	5.51	4.54	4.39
01-72	5.54	4.55	4.52
02-01	6.32	6.00	5.57
03-43	7.48	5.68	5.59
KR64300 ^a	6.30	4.00	4.00
KR64301 ^b	6.15	4.05	4.31
LAF237 ^c	6.10	4.55	4.46
MK0431 ^d	6.32	4.03	4.00

^{a,b}Our experimental team synthesized (Ref. 10).

^{c,d}Lately clinical state compounds.

^eRef. 9.

structed by modifying the structures. The molecular-modeling software package Sybyl7.1 was used to construct these compounds. Partial atomic charges were calculated by the Gasteiger–Huckel method and energy minimizations were carried out using the Tripos force-field¹⁴ with a distance-dependent dielectric and the Powell conjugate gradient algorithm.

The 3D structure of DPP4 enzyme is well known, but those of DPP8 and DPP9 are not relatively known. DPP8 with 882 amino acid residues (AA) and DPP9 consisting of 971 AA show sequence homology of 51%¹⁵ and 26%¹⁶ with DPP4 (766 AA) at the atomic level, respectively. To construct the 3D structures for the DPP8 and DPP9 enzymes, an automated protein homology-modeling server, SWISS-MODELER,¹⁷ was used, and molecular dynamics simulation techniques using CHARMM32b1 force-field¹⁸ were used in an implicit solvent model with distance-dependent dielectric constant. In Figure 1, the characteristics of DPP4 active site were analyzed and were found to consist of three parts (S1, S2, S3 sites) being shown by three white boxes including the catalytic residues, S630, N710, and H740, and the ionic interaction site (E205, E206) following S3 sites consisting of S209, F357, and R358. According to the 3D structure of DPP8 and DPP9 obtained from the homology-modeling study, the S1 site with different DPP isozymes is nearly the identical in terms of the residue composition, while the pocket size of the S1 site is slightly different. The S2 site and the S1' site

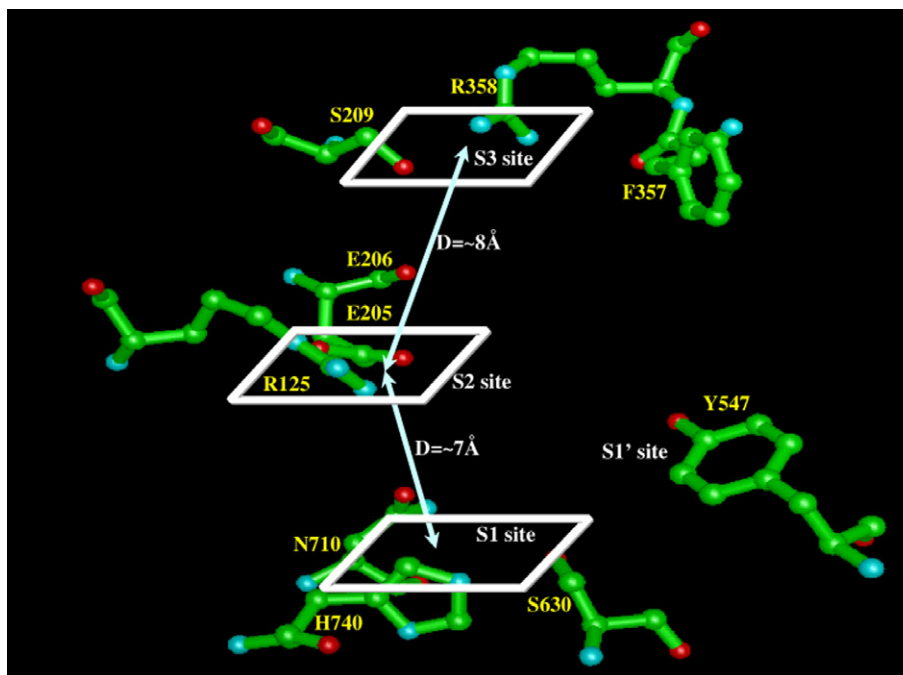


Figure 1. The characteristics of DPP4 active site. The major three parts for the ligand binding are symbolized as S1 including catalytic residues, S2 with ionic interaction sites, and S3.

are slightly different in terms of the residue composition or conformation. In particular, the S3 site is greatly different for each isozyme. To validate the DPP4 isozyme structures obtained from above procedure and also to get an alignment for 3D-QSAR, we carried out a docking study for a training set, 43 compounds. At first, we manually docked a training set into the active sites of DPP4, DPP8, and DPP9, using an in-house window-based modeling program, WinPro. For docking, we used 1X70.pdb as reference complex structure. Then, we calculated the binding score value using Sybyl7.1/Chem_Score¹⁹ method with relax molecule algorithm. We repeated these processes until we obtained a good model having high correlation between the binding score (Chem_Score) and the inhibitory activity (Fig. 2). The aligned structures based on this good model are shown in Figure 3.

For the 3D-QSAR studies, CoMFA, a sp^3 carbon atom and a +1 net charge atom were used as the steric and electronic field energy probes, respectively. The Tripos force-field with a distance-dependent dielectric constant at all interactions in a regularly spaced (2Å) grid was used for the steric and electronic interactions. The energy cutoff was set to 30 kcal/mol, and a regression analysis was carried out using the full cross-validated partial least squares (PLS) methods, incorporating leave-one-out, with the CoMFA standard options for scaling variables. The minimum sigma was set to 2.0 kcal/mol to improve the signal-to-noise ratio by omitting the lattice points whose energy variation was below this threshold. The final model obtained from the non-cross-validated conventional analysis was developed with the optimal number of components equal to that showing the highest q^2 .

A PLS analysis for 43 DPP4, DPP8, and DPP9 inhibitors was carried out, and the results are shown in Table 3. The predicted activities of a test set including 10 compounds are represented in Table 4. The correlation plots of the predicted activities (predicted pIC_{50}) versus their experimental activities (observable pIC_{50}) are depicted in Figure 4a–c for DPP4, DPP8, and DPP9, respectively. Table 3 and Figure 4 demonstrate that the predicted activities by the CoMFA model are in good agreement with the experimental data, showing that the constructed CoMFA model is reliable.

A 3D-coefficient contour interaction map of the CoMFA results is shown in Figure 5(a–c) for DPP4, DPP8, and DPP9, respectively. This demonstrates regional variations in the steric and electrostatic characteristics of the structural features of the different molecules contained in the training set that increase or decrease the biological activity. In these contour maps, the green regions indicate areas where the sterically bulkier group enhances the enzymatic inhibitory activities, and the yellow regions show that the sterically less bulky group is favorable to inhibitory activity. Blue regions suggest areas where more positively charged groups are favorable to enzymatic inhibitory activity, while red regions represent the more negatively charged groups that are favorable to activity.

The important binding sites S1, S2, and S3 are explained in the aforementioned section (Fig. 1). The CoMFA contour map showed that there are favorable regions for steric interaction, indicated as the green-colored contour around the S1 site in DPP8 and DPP9, which shows different phenomena compared to DPP4. As another study showed,²⁰ the S1 pocket size is smaller in DPP4

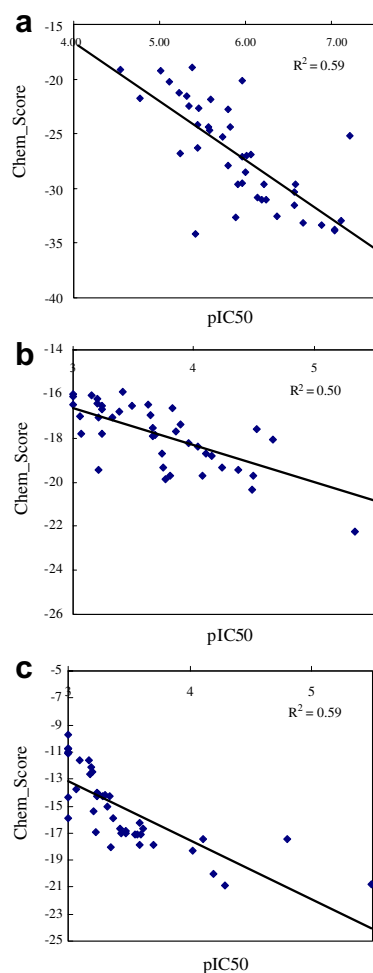


Figure 2. Chem_Score obtained for 43 compounds in active sites of (a) DPP4, (b) DPP8, and (c) DPP9.

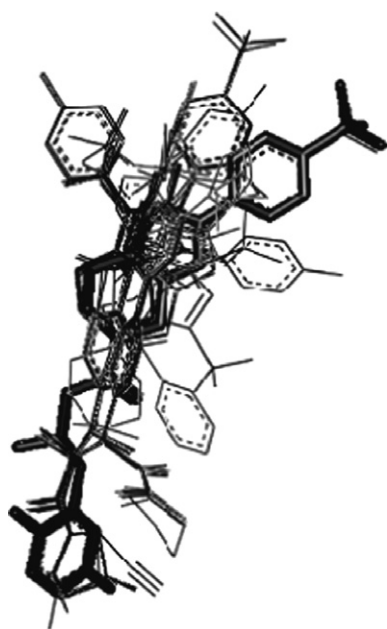


Figure 3. Alignment of 53 derivatives (a training set and a test set) for 3D-QSAR studies.

Table 3. The results of CoMFA calculations

CoMFA parameters	DPP4	DPP8	DPP9
q^2 (CV correlation coefficient)	0.68	0.58	0.68
N (number of components)	5	6	6
r^2 (correlation coefficient)	0.96	0.98	0.97
F (F-ratio)	169.85	264.34	180.27
S:E (steric:electrostatic)	47.0:53.0	42.7:57.3	45.9:54.1
r_{bs}^2 (bootstrapping coefficient)	0.98	0.98	0.98

Table 4. Prediction of 10 compounds in a test set

Test set	DPP4-pred	DPP8-pred	DPP9-pred
01-54	5.62	4.78	4.56
01-60	5.92	4.87	4.38
01-67	5.75	5.05	4.60
01-72	5.72	4.58	4.50
02-01	5.40	4.85	4.86
03-43	6.86	5.06	4.36
KR64300	5.80	4.61	4.35
KR64301	5.72	4.21	4.25
LAF237	5.88	5.43	5.36
MK0431	5.99	4.93	4.44

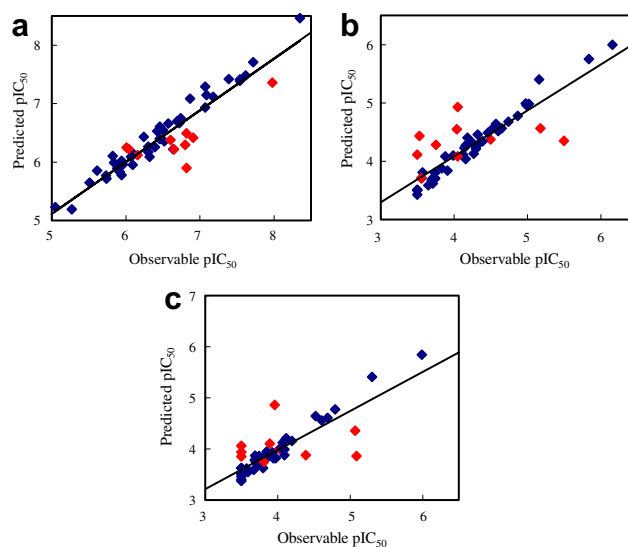


Figure 4. The correlation plots of predicted pIC_{50} versus observable pIC_{50} from training set (filled blue square) and test set (filled red diamond) for (a) DPP4, (b) DPP8, and (c) DPP9 systems.

compared to DPP8 and DPP9. Noticeably, the positions of the S1' site differ greatly in DPP4 and its isozymes. The S1' sites of DPP8 and DPP9 need less bulky and positively charged groups, while those of DPP4 prefer comparatively negatively charged groups. The positions between the S2 site and the S3 site are favorable to less bulky groups in DPP8 or DPP9, differing from DPP4. In contrast, the S3 sites in DPP8 and DPP9 are acceptable to bulkier groups compared to DPP4. According to unpublished data obtained by the authors from an X-ray co-crystal and from another paper,²⁰ the S3 site, in particular around F357 (DPP4), plays an important role in enhancing the selectivity to DPP8. Accordingly, it was expected that KR64300 and KR64301 with six- and seven-membered cyclic hydrazines, which

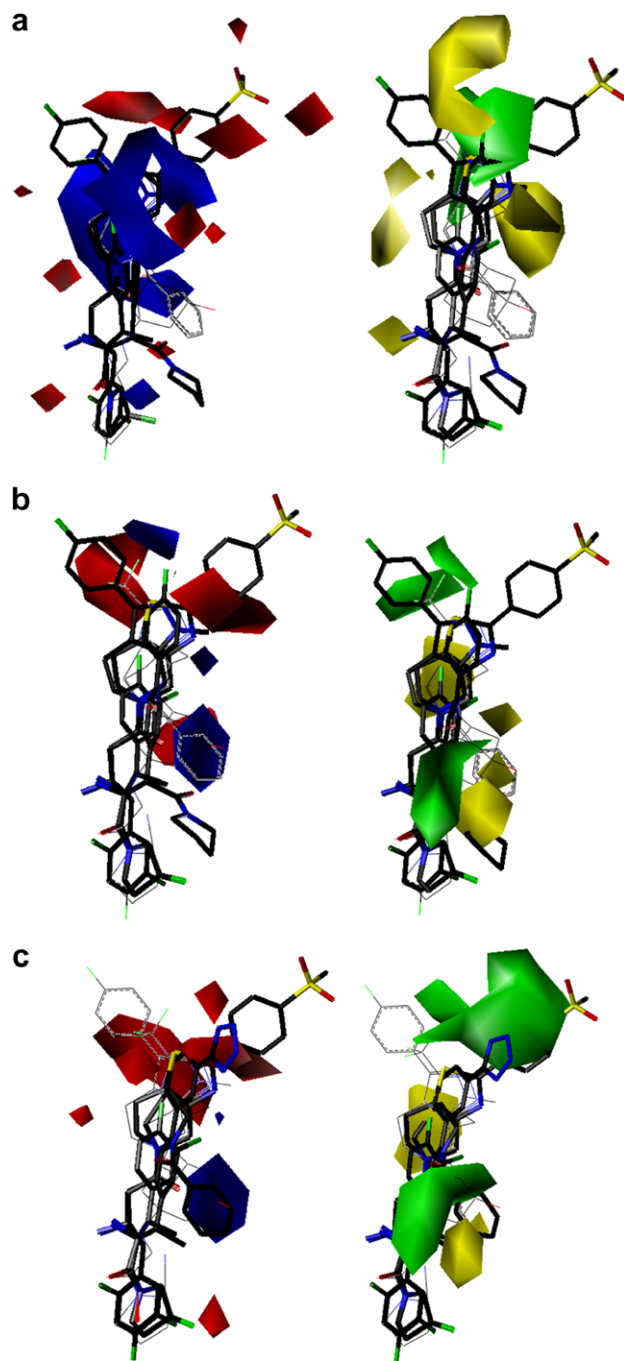


Figure 5. CoMFA contour maps. (a) DPP4, (b) DPP8, and (c) DPP9 systems; (left) electrostatic, (right) steric map. Sterically favored areas in green color; sterically unfavored area in yellow. Blue colored region favored positive potential field; red colored region favored negative potential field.

obtain less bulky S3 site substituents but interact with F357 in the S3 site and also possibly interact with the S1', would show a good selectivity. The result of the prediction from the CoMFA model, as shown in Table 4, met the expectations. Evidently, the experimental IC_{50} values of the KR64300 and KR64301 compounds for DPP8 and DPP9 inhibitory activity agreed with the above results. Not having S3 site substituents, the thiazolidide 02-02 and 02-03 compounds showed less favorable selectivity. In Figure 6, the important residues

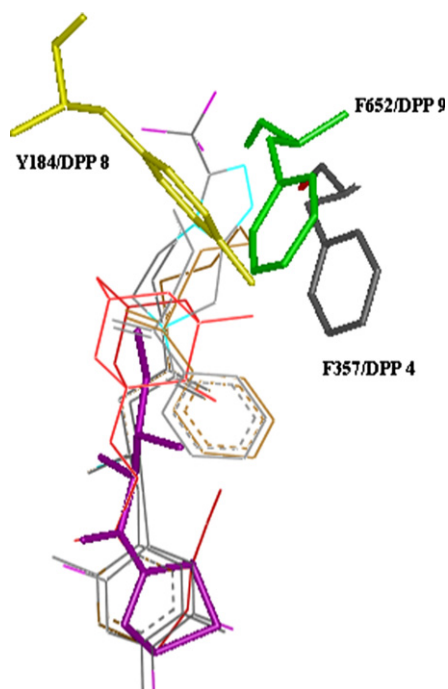


Figure 6. The important residues in S3 sites of DPP4, DPP8, and DPP9. The shown inhibitors are MK0431 (mixed color), KR64300 (gray), KR64301 (brown), LAF23 7 (red), and 02-02 (magenta).

of DPP4 and its isozymes are depicted, suggesting that the Y184 and F652 residues of DPP8 and DPP9 are positioned downward from the S3 pocket. Hence, these residues cause the outside part of the S3 pocket of DPP8 and DPP9 to become shallower, while causing the inside of the S3 pocket to broaden. As shown in the CoMFA contour map, the outside of the S3 pocket in DPP4 allows larger groups to enhance the activity, but in the case of DPP8 and DPP9 this is not so. On the other hand, the inside position of the S3 pocket in DPP4 prefers the smaller group, while in the opposite is true for DPP8 and DPP9. Equally, in Figure 6, compounds identical to thiazolidide 02-02 (magenta), which only occupies S1 and S2 sites, have no selective activity. However, compounds such as MK0431, KR64300, and KR64301, which bind to the outside position of the S3 site, show very selective inhibitory activity.

In this study, a highly predictive CoMFA model for selective DPP4 inhibitors was obtained. The reliable model showed leave-one-out cross-validation q^2 and conventional r^2 values of 0.68 and 0.96 for DPP4 inhibitors, 0.58 and 0.98 for DPP8 inhibitors, and 0.68 and 0.97 for DPP9 inhibitors, respectively. The reliability of the CoMFA model was verified by the compounds in a test set, including the newly synthesized six- and seven-membered cyclic hydrazines. Additionally, the consistency between the 3D structure of protein and the CoMFA contour map indicates the robustness of the 3D-QSAR model. According to this study, in order to obtain selective DPP4 inhibitors compared to the isozymes, the interaction of the inhibitors with the S3 site and S1' site in DPP4 should be carefully considered. The proposed newly synthesized compounds, KR64300 and KR64301,

interact well with the aforementioned sites, thus showing excellent selectivity. In addition, by combining the more refined 3D structures of DPP8 and DPP9 with 3D-QSAR, in terms of the atomic details, inhibitors more active to DPP4 than to KR compounds and more selective to DPP8 and DPP9 enzymes are sought by the authors.

Acknowledgment

This research was supported by the Center for Biological Modulators of the 21st Century Frontier R&D Program, the Ministry of Science and Technology, Korea.

References and notes

- (a) Kieffer, T. J.; McIntosh, C. H. S.; Pederson, T. A. *Endocrinology* **1995**, *136*, 3585; (b) Deacon, C. F.; Nauck, M. A.; Toft-Nielsen, M.; Pridal, L.; Willms, B.; Holst, J. J. *Diabetes* **1995**, *44*, 1126; (c) Mentlein, R. *Regulatory Pept.* **1999**, *85*, 9.
- (a) Villhauer, E. B.; Coppola, G. M.; Hughes, T. E. *Annu. Rep. Med. Chem.* **2001**, *36*, 191; (b) Wiedeman, P. E.; Trevillyan, J. M. *Curr. Opin. Invest. Drugs* **2003**, *13*, 499; (c) Weber, A. E. E. *J. Med. Chem.* **2004**, *47*, 4135.
- (a) Ahren, B.; Holst, J. J.; Martensson, H.; Balkan, B. *Eur. J. Pharmacol.* **2000**, *404*, 239; (b) Deacon, C. F.; Hughes, T. E.; Joist, J. J. *Diabetes* **1998**, *47*, 764; (c) Pospisilik, J. A.; Stafford, S. G.; Demuth, H.-U.; Brownsey, R.; Parkhous, W.; Finegood, D. T.; McIntosh, D. H. S.; Pederson, R. A. *Diabetes* **2002**, *51*, 943.
- (a) Deacon, D. F.; Holst, J. J. *Int. J. Biochem. Cell Biol.* **2006**, *38*, 831; (b) Triplitt, C.; Wright, A.; Chiquett, E. *Pharmacotherapy* **2006**, *26*, 360; (c) Augustyn, K.; Van der Veken, P.; Haemers, A. *Expert Opin. Ther. Patents* **2005**, *15*, 1387; (d) Hunziker, D.; Hennig, M. *Peters J. Curr. Topics Med. Chem.* **2005**, *5*, 1623.
- Villhauer, E. B.; Brinkman, J. A.; Naderi, G. B.; Burkey, B. F.; Dunning, B. E.; Prasad, K.; Mangold, B. L.; Russell, M. E.; Hughes, T. E. *J. Med. Chem.* **2003**, *46*, 2774.
- Kim, D.; Wang, L.; Beconi, M.; Eiermann, G. J.; Fisher, M. H.; He, H.; Hickey, G. J.; Kowalchick, J. E.; Leiting, B.; Lyons, K.; Marsilio, F.; McCann, M. E.; Patel, R. A.; Petrov, A.; Scapin, G.; Patel, S. B.; Roy, R. S.; Wu, J. K.; Wyvratt, M. J.; Zhang, B. B.; Zhu, L.; Thornberry, N. A. *J. Med. Chem.* **2005**, *48*, 141.
- Rosenblum, J. S.; Kozarich, J. W. *Curr. Opin. Chem. Biol.* **2003**, *7*, 496.
- Lankas, G.; Leiting, B.; Sinha Roy, R.; Eiermann, G.; Biftu, T.; Kim, D.; Ok, H.; Weber, A. E.; Thornberry, N. A. *Diabetes* **2004**, *53*, A2.
- (a) Ashton, W. T.; Sisco, R. M.; Dong, H.; Lyons, K. A.; He, H.; Doss, G. A.; Leiting, B.; Patel, R. A.; Wu, J. K.; Marsilio, F.; Thornberry, N. A.; Weber, A. E. *Bioorg. Med. Chem. Lett.* **2005**, *15*, 2253; (b) Xu, J.; Wei, L.; Mathvink, R.; He, J.; Park, Y. J.; He, H.; Leiting, B.; Lyons, K. A.; Marsilio, F.; Patel, R. A.; Wu, J. K.; Thornberry, N. A.; Weber, A. E. *Bioorg. Med. Chem. Lett.* **2005**, *15*, 2533; (c) Edmondson, S. D.; Mastracchio, A.; Duffy, J. L.; Eiermann, G. J.; He, H.; Ita, I.; Leiting, B.; Leone, J. F.; Lyons, K. A.; Makarewicz, A. M.; Patel, R. A.; Petrov, A.; Wu, J. K.; Thornberry, N. A.; Weber, A. E. *Bioorg. Med. Chem. Lett.* **2005**, *15*, 3048.
- Ahn, J. H.; Shin, M. S.; Jung, S. H.; Kang, S. K.; Kim, R. K.; Rhee, S. D.; Kang, N. S.; Kim, S. Y.; Sohn, S. K.; Kim, S. G.; Jin, M. S.; Lee, J. O.; Cheon, H. G.; Kim, S. S. *Bioorg. Med. Chem. Lett.* **2007**, *17*, 2622.
- Kim, D.; Wang, L.; Beconi, M.; Eiermann, G. J.; Fisher, M. H.; He, H.; Hickey, G. J.; Kowalchick, J. E.; Leiting, B.; Lyons, K.; Marsilio, F.; McCann, M. E.; Patel, R. A.; Petrov, A.; Scapin, G.; Patel, S. B.; Roy, R. S.; Wu, J. K.; Wyvratt, M. J.; Zhang, B. B.; Zhu, L.; Thornberry, N. A.; Weber, A. E. *J. Med. Chem.* **2005**, *48*, 141.
- Thoma, R.; Loeffler, B.; Stihle, M.; Huber, W.; Ruf, A.; Henning, M. *Structure* **2003**, *11*, 947.
- Engel, M.; Hoffmann, L.; Wagner, M.; Wermann, M.; Heiser, U.; Kiefersauer, R.; Huber, R.; Bode, W.; Demuth, H. U.; Brandstetter, H. *Proc. Nat. Acad. Sci. U.S.A.* **2003**, *100*, 5063.
- Clark, M.; Cramer, R. D.; Leach, A. R.; Taylor, R. *J. Mol. Biol.* **1997**, *267*, 727.
- Abbott, C. A.; Yu, D. M.; Woollatt, E.; Sutherland, G. R.; McCaughan, G. W.; Gorrell, M. D. *Eur. J. Biochem.* **2000**, *267*, 6140.
- Ajami, K.; Abbott, C. A.; McCaughan, G. W.; Gorrell, M. D. *Biochim. Biophys. Acta* **2004**, *1679*, 18.
- (a) Schwede, T.; Kopp, J.; Guex, N.; Peitsch, M. C. *Nucleic Acids Res.* **2003**, *31*, 3381; (b) Guex, N.; Peitsch, M. C. *Electrophoresis* **1997**, *18*, 2714; (c) Peitsch, M. C. *BioTechnology* **1995**, *13*, 658.
- Brooks, B. R.; Bruccoleri, R. E.; Olafson, B. D.; States, D. J.; Swaminathan, S.; Karplus, M. *J. Comp. Chem.* **1983**, *4*, 187.
- Eldridge, M. D.; Murray, C. W.; Auton, T. R.; Paolinite, G. V.; Mee, R. P. *J. Comp.-Aid. Mol. Des.* **1997**, *11*, 425.
- Lu, I. L.; L, S. J.; Tsu, H.; Wu, S. Y.; Kao, K. H.; Chien, C. H.; Chang, Y. Y.; Chen, Y. S.; Cheng, J. H.; Chang, C. N.; Chen, T. W.; Chang, S. P.; Chen, X.; Jiaang, W. T. *Bioorg. Med. Chem. Lett.* **2005**, *15*, 3271.